

See discussions, stats, and author profiles for this publication at: <https://www.researchgate.net/publication/259107191>

Shear Flow Controlled Morphological Polydispersity of Amphiphilic ABA Triblock Copolymer Vesicles

ARTICLE in LANGMUIR · NOVEMBER 2013

Impact Factor: 4.46 · DOI: 10.1021/la404186u · Source: PubMed

CITATION

1

READS

34

4 AUTHORS, INCLUDING:



Jie Cui

Changchun Institute of Applied Chemistry

15 PUBLICATIONS 93 CITATIONS

[SEE PROFILE](#)



Yutian Zhu

Chinese Academy of Sciences

43 PUBLICATIONS 356 CITATIONS

[SEE PROFILE](#)

Shear Flow Controlled Morphological Polydispersity of Amphiphilic ABA Triblock Copolymer Vesicles

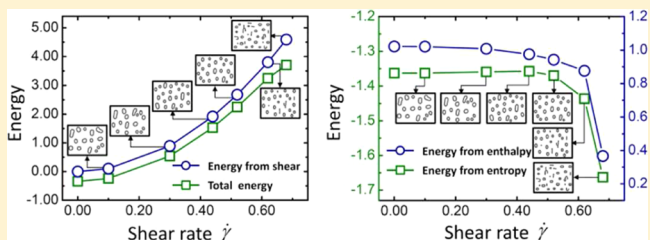
Jie Cui,[†] Jiangping Xu,^{†,‡} Yutian Zhu,[†] and Wei Jiang^{*,†}

[†]State Key Laboratory of Polymer Physics and Chemistry, Changchun Institute of Applied Chemistry, Chinese Academy of Sciences, Changchun 130022, P. R. China

[‡]University of Chinese Academy of Sciences, Beijing 100049, P. R. China

Supporting Information

ABSTRACT: Self-assembled polymeric aggregates are generally polydisperse in morphology due to the existence of many metastable states in the system. This shortcoming becomes a bottleneck for preparing high quality self-assembled polymeric materials. An important concern is the possibility of controlling morphological polydispersity through the modulation of the metastable states. In this study, both simulative and experimental results show that the metastable states can be modulated. As a typical example, the morphological polydispersity of amphiphilic ABA triblock copolymer vesicles have been successfully controlled by shear flow. A higher shear rate results in more uniform and smaller vesicles. However, if the shear rate is extremely high, small spheres and short rods can be observed. These findings not only give a deeper insight into the metastable behavior of self-assembled polymeric aggregates but also provide a new strategy for improving the uniformity of vesicles.



1. INTRODUCTION

Uniformity is a prime requirement to realize the full potential of polymeric assemblies. However, self-assembled polymeric aggregates are generally polydisperse in shape and size.^{1–10} This morphological polydispersity limits their applications in many fields. For example, the regulation of morphology, size, and size distribution of vesicles is very important for improving their performance in applications such as the delivery and controlled release of drug and catalyst.^{11–19} The nanocapsule size is a major factor determining the *in vivo* fate and biodistribution of the capsules.²⁰ Vesicles with a proper size, e.g. less than ~100 nm in diameter, can avoid renal exclusion and reticuloendothelial system and have enhanced endothelial cell permeability in the vicinity of solid tumor.¹³ Too small or too large vesicles are not appropriate for biological applications. Thus, the size distribution of the polymer vesicles is crucial in achieving modulated drug delivery with remarkable efficacy.¹⁴ The preparation of vesicles with regular morphology and narrow size distribution has gained increasing interest among researchers. However, in both simulations and experiments, one can always find a wide range of morphologies and size distributions of vesicles in solution.^{3,7,21–23} The origin of self-assembly tightly specifies the wall thickness of the resulting vesicle. However, both for polymer vesicles and phospholipids, no mechanism strongly selects for the overall size.^{4,24,25} Therefore, the size distribution of vesicles is very polydisperse. Current synthetic and assembly methods typically produce such polydisperse vesicles. The coexistence of vesicles with many different sizes has become a fatal drawback that limits vesicle performance in practical applications.¹⁰

To the best of our knowledge, only several contributions have been conducted on the control of the size distribution of polymer vesicles.^{24,26–32} Holowka et al. reported a liposome-based extrusion technique to finely adjust the polypeptide vesicles due to the high degree of membrane fluidity.²⁹ Xu and co-workers recently used a membrane-extrusion emulsification approach to control the size and size distribution of polymer nanocapsules.³² The general problem of these techniques is that the size and size distribution of the nanocapsules heavily depend on the filter membrane pore size. Recently, the microfluidic fabrication technique was introduced by Shum et al. to prepare monodisperse polymersomes with biocompatible and biodegradable diblock copolymers.³¹ Dong et al. introduced a novel self-templating strategy to prepare uniform and biocompatible nanocapsules.²⁸ Howse et al. reported a method that combines photolithography and molecular self-assembly for the production of giant polymer vesicles with controlled size distributions, which may have applications in drug and gene delivery.²⁴ However, these techniques are complicated and time-consuming in template fabrication. Thus far, it remains a challenge to develop methods to produce monodisperse vesicles from synthetic block copolymers.¹⁰

Eisenberg et al. once proposed that the polydispersity inherent in macromolecular samples is one possible factor that contributes to the coexistence of micelles with disparate morphologies, such as sphere, rod, lamellar, vesicle, and so

Received: October 29, 2013

Revised: November 28, 2013

Published: November 30, 2013

on.³³ Later, Liang and Jiang et al. revealed, by both experiments and simulations, that even though the macromolecular weights are monodisperse, the coexistence behavior still exists due to the existence of many metastable states in the system.^{23,34,35} Thus, for polymer solution with vesicles of many different sizes, we can reasonably conceive that the vesicle size polydispersity is originated from the many metastable states existing in the system. It implies that the size polydispersity of vesicles cannot be highly improved until the metastable states are well tuned. The possibility of tuning the metastable states in solution system becomes a key problem that we have to face. Herein, we investigated the effects of shear rate of a uniform shear field on the metastable states of a solution system through theory and simulation and verified the simulation prediction by experiment. The purpose of this study is to determine an effective way to modulate the metastable states and thereby control the morphological polydispersity of the assemblies.

2. THEORY AND SIMULATION SECTION

The SCFT simulation was employed because it can give the equilibrium morphologies corresponding to the minimum points (i.e., metastable states) on the free energy landscape.³⁶ Moreover, it has proven to be a powerful tool to study the self-assembly of polymer chains with various architectures such as block, star, and brush. For the ABA triblock copolymer solution system, the copolymer and solvent S are involved in volume V. The volume fraction of the triblock copolymer in the dilute solution is f_p . Incompressibility is assumed in this mixture system. For such a system without shear flow, the free energy density for a single chain is given by

$$F_{\text{SCF}} \equiv \frac{NF}{\rho_0 V k_B T} = -f_p \ln(Q_p/f_p V) - Nf_S \ln(Q_s/f_s V) \\ - 1/V \int d\vec{r} \left[\sum_{\alpha} \omega_{\alpha}(\vec{r}) \phi_{\alpha}(\vec{r}) + P(\vec{r})(1 - \sum_{\alpha} \phi_{\alpha}(\vec{r})) \right] \\ + 1/V \int d\vec{r} \left[\sum_{\alpha \neq \beta} \chi_{\alpha\beta} N \phi_{\alpha}(\vec{r}) \phi_{\beta}(\vec{r}) / 2 \right] \quad (1)$$

where N is the total length of the block copolymer chain, $\chi_{\alpha\beta}$ is the Flory–Huggins interaction parameters between species α and β , and $\phi_{\alpha}(\vec{r})$ is the density fields of species α ($\alpha = A, B$, and S). $P(\vec{r})$ is the well-known Lagrange multiplier which enforces the incompressibility. $Q_p = \int d\vec{r} q(\vec{r}, 1)$ is the partition function of a single polymer chain in an effective chemical potential field $\omega_A(\vec{r})$ and $\omega_B(\vec{r})$. $Q_s = \int d\vec{r} \exp(-\omega_s(\vec{r})/N)$ is the partition function of the solvent in an effective chemical potential field $\omega_s(\vec{r})$. $q(\vec{r}, s)$ is the propagator that gives the probability of finding segment s at position \vec{r} , and it satisfies the modified diffusion equation $\partial q(\vec{r}, s) / \partial s = \nabla^2 q(\vec{r}, s) - \omega(\vec{r}, s) q(\vec{r}, s)$. Minimizing the free energy leads to a set of SCFT equations that can be solved numerically by real-space method.^{37–39} To mimic dilute solution, the volume fraction of the ABA triblock copolymer was fixed at $f_p = 0.1$. The total chain length N equals 17 with the chain length of each block being 1, 15, and 1, respectively.

To study whether the metastable behavior can be modulated and the morphological polydispersity can be consequently controlled, shear field was introduced in this study because it is one of the most important external fields and widely used in experiments. According to the work of An and Wolf and Sun et al.,^{40,41} we can obtain the local energy arising from shear flow

(denoted by) for the linear ABA triblock copolymer solution ΔG_{shear} system as follows:

$$\Delta G_{\text{shear}}(\vec{r}) = k_0 \dot{\gamma}^{2-C_0} - \sum_{\alpha=A,B,S} k_{\alpha} \phi_{\alpha}(\vec{r}) \dot{\gamma}^{2-C_{\alpha}} \quad (2)$$

The SCFT free energy with shear flow can thus be expressed as $F_{\text{SCF}}^{\text{shear}} = F_{\text{SCF}} + 1/V \int d\vec{r} \Delta G_{\text{shear}}(\vec{r})$. In eq 2, $\dot{\gamma}$ is the shear rate. k_0 and k_{α} are parameters relating to shear compliance and viscosity of the polymer solution and pure components α , respectively.⁴¹ C_0 and C_{α} are related to the viscosity variations with the shear rate. Considering that the polymer solution is dilute, we ignored the hydrodynamic difference between the dilute solution and the pure solvent in this study (i.e., $k_0 = k_s$). According to numerous calculated results obtained from eq 2 at various k_0 , k_{α} , φ_{α} and $\dot{\gamma}$ (for simplicity, $C_0 = C_{\alpha} = 0$), we found that k_0 should be larger than k_A and k_B . In the current work, we chose $k_0 = k_s = 160$, $k_A = 70$, and $k_B = 60$. More details about the simulation method are given in the Supporting Information.

3. EXPERIMENTAL SECTION

3.1. Materials. The amphiphilic triblock copolymer used in this study was poly(4-vinylpyridine)-*b*-polystyrene-*b*-poly(4-vinylpyridine) (P4VP₄₃-*b*-PS₃₆₆-*b*-P4VP₄₃, the subscripts indicate the number of repeat units of the blocks, $M_n = 47\,000$ g/mol, PDI = 1.10, Polymer Source). Dioxane was the common solvent, and the mixture of deionized water and anhydrous methanol (volume ratio 2:3) was used as selective solvent.

3.2. Preparation of the Polymeric Vesicles. The method we used to prepare polymeric vesicles was described elsewhere in the literature.⁴² The triblock copolymer (30 mg) was first dissolved in 3.00 mL of dioxane. Then the polymer solution was transferred to the Couette cell which offers an approximately uniform flow field (details in Supporting Information) and sheared under a preset shear rate for another 2 h. Mixed selective solvent (1.05 mL) was slowly added to the solution at a rate of 0.05 mL/30 s to induce the aggregation of the PS blocks. After being sheared for another 24 h at room temperature, 0.25 mL of the solution was quickly added to 5 mL of deionized water to quench the aggregate morphology. Subsequently, the resulting solution was dialyzed against deionized water (pH = 4) for 4 days to remove the organic solvent from the vesicle solution.

3.3. Characterization. The morphologies of the aggregates were collected from a JEOL JEM-1011 transmission electron microscope (TEM) operated at an acceleration voltage of 100 kV. A drop of dialyzed vesicle aqueous solution (0.4 mg mL⁻¹) was placed onto a TEM copper grid covered by a polymer support film precoated with carbon thin film. After 5 min, excess solution was blotted away using a strip of filter paper. Then the samples were dried in atmosphere at room temperature for 1 day before observation. No stained process was needed.

The size and the size distribution of the vesicle were investigated by dynamic laser scattering (DLS) with Wyatt DynaPro Nanostar instrument at a fixed angle of 90° at 25 °C. The wavelength of the laser is 658 nm. The concentration of the vesicle solution is 0.08 mg mL⁻¹. The hydrodynamic radius (R_h) and polydispersity index (PDI) are given by cumulant analysis of the DLS intensity autocorrelation function, while the size distribution curves are given by the CONTIN method. A smaller PDI value indicates a narrower or more uniform size distribution of the vesicles. The R_h and PDI reported in this study represent the average results of three repeated experiments.

4. RESULTS AND DISCUSSION

In simulations, different homogeneous initial states are generated by using different random number generators while the composition of the system and the copolymer density and its initial fluctuation amplitude remain unchanged. Meanwhile, the Flory–Huggins interaction parameters χ_{AS} was set as

negative and χ_{BS} as positive, corresponding to their amphiphilic nature. The parameter χ_{AB} was set as positive to mimic the incompatibility between blocks A and B. To obtain vesicles, we set the Flory–Huggins interaction parameters to be $\chi_{AB} = 18.0$, $\chi_{AS} = -23.0$, and $\chi_{BS} = 22.1$. Figures 1a,b show the 3D SCFT

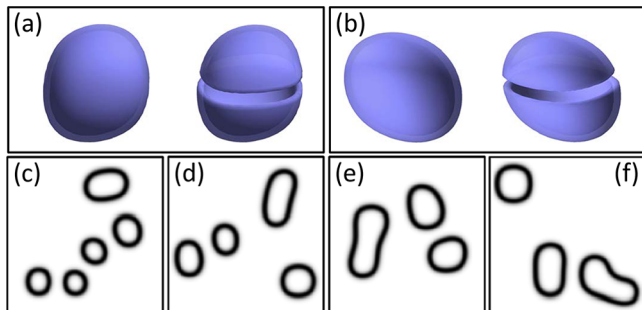


Figure 1. (a, b) Aggregates obtained in 3D simulation from different initial states. To confirm that the aggregates are vesicles, corresponding cross sections were also given in (a) and (b), respectively; (c–f) vesicles obtained in 2D simulation from different initial states. The interaction parameters used in 2D are the same as those used in 3D.

simulation results for two different initial states in the case of $\dot{\gamma} = 0$ (i.e., without shearing). It is clear that the ABA triblock copolymers self-assemble into vesicle. Figures 1c–f show the 2D simulation results under the same condition as those used in the 3D simulation. As all the simulation parameters remain unchanged, we can know that the loops in Figures 1c–f are corresponding to the vesicles in 3D. Because of the limit of the simulation scale, only a few vesicles can be obtained in a 3D lattice. However, a large number of vesicles are needed in order to study their morphological polydispersity. Therefore, we performed our simulation in a 2D lattice with the size of 128×128 in this paper. Periodic boundary condition was imposed in both x and y directions. Obviously, Figure 1 shows us that the vesicle morphology varies with initial state. As the simulation results are corresponding to the minimum points (i.e., metastable states) on the free energy landscape and the macromolecular weight of the triblock copolymer is monodisperse, we can conclude that the morphological polydispersity results from the existence of many metastable states in the system.

Figure 2 presents the simulation results of the vesicles formed by ABA triblock copolymers at different shear rates. To obtain more vesicles for statistics, more than 15 initial states

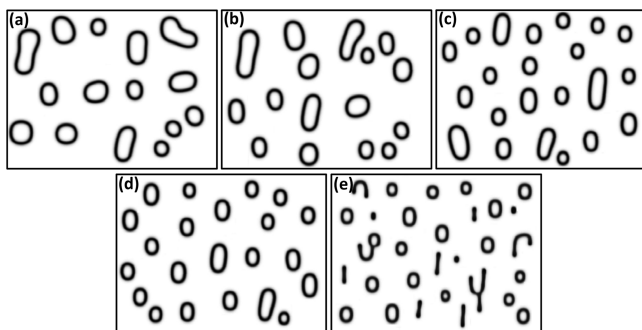


Figure 2. Vesicles obtained from SCFT simulations at different shear rates: (a) $\dot{\gamma} = 0.10$; (b) $\dot{\gamma} = 0.30$; (c) $\dot{\gamma} = 0.44$; (d) $\dot{\gamma} = 0.52$; (e) $\dot{\gamma} = 0.68$.

were performed (hence more than 50 vesicles) at a given shear rate. Several big vesicles coexist with relatively small vesicles when the shear rate is as low as 0.10 (Figure 2a). As the shear rate increases, the vesicles gradually diminish in size (Figures 2b,c). When the shear rate is increased to 0.52 (Figure 2d), the big vesicles disappear, leaving only small vesicles. It should be noted that when the shear rate is higher than 0.52, a small amount of nonvesicle structures (such as short rods, spheres) begin to appear. However, when the shear rate increases to 0.68 (Figure 2e), a large number of nonvesicle structures were obtained from simulation. What is more important is that the uniformity of the vesicles can be considerably improved by increasing the shear rate from 0.10 to 0.52. For quantitative study, the number-averaged size \bar{S}_n and size distribution of the vesicles were calculated. The vesicle size is represented by the area (in unit of R_g^2 , where R_g is the radius of gyration of the triblock copolymer) that it occupies and measured by a common graphic tool. The statistical results are given in Figure 3. From Figure 3 we can observe that the averaged vesicle size

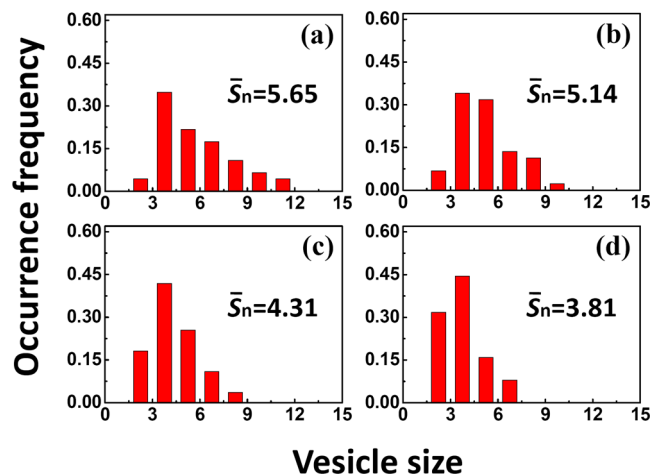


Figure 3. Averaged vesicle size and size distribution at different shear rates: (a) $\dot{\gamma} = 0.10$; (b) $\dot{\gamma} = 0.30$; (c) $\dot{\gamma} = 0.44$; (d) $\dot{\gamma} = 0.52$.

decreases from 5.65 to 3.81 with the increase of shear rate. The vesicle size distribution becomes narrow as the shear rate increases, which indicates that the vesicles tend to be uniform. To further reveal the effect of the shear rate on the vesicle size, the variation of size polydispersity index (PDI) of the vesicles, and the number-averaged vesicle size, with the shear rate are plotted in Figure 4. From Figure 4 we can find that the averaged vesicle size \bar{S}_n decreases with the increase of shear rate. Meanwhile, the vesicle size PDI becomes lower as the shear rate increases. Therefore, we conclude that the polydispersity of vesicles can be controlled by shear flow. The higher the shear rate, the more uniform vesicles can be obtained.

We know that the SCFT simulation can give the equilibrium morphologies corresponding to numerous metastable states on the free energy landscape. Our simulation results (Figure 1) show that the existence of numerous metastable states is the reason that vesicles have various sizes, which results in the wide size distribution of vesicles. However, when the shear field is applied to the system, larger vesicles disappear (Figure 2). This indicates that the metastable states of the system can be tuned by shear field. The decrease in the number of metastable states arising from shear field can lead to narrower size distribution. Here, we would like to note that the shear rate used in the

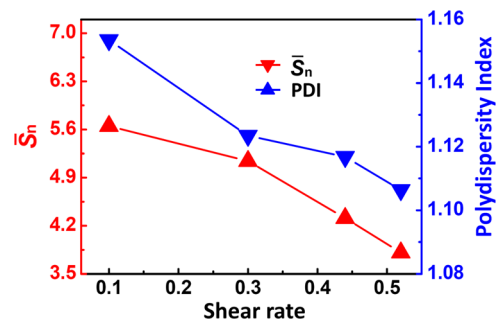


Figure 4. Variation of number-averaged size and size PDI of vesicles with the shear rate. The PDI were calculated according to $\text{PDI} = \bar{S}_w / \bar{S}_n$, where the weight-averaged size of vesicles was calculated by $\bar{S}_w = \sum n_i S_i^2 / \sum n_i S_i$ and the number-averaged size by $\bar{S}_n = \sum n_i S_i / \sum n_i$.

simulation is a reduced parameter, and its value cannot be directly compared with the actual shear rate in the experiment.

Consequently, another question that we are concerned about is whether the above simulation results can be supported by the experimental results. In the simulation, a uniform shear field was applied to conduct quantitative calculation. However, in experiments, the shear field is generally supplied by a stirring bar. The stirring rate reportedly showed considerable influence on the micelle morphology.^{43–46} For example, our previous works have shown that the stirring rate influences the formation of toroidal micelles of ABA triblock copolymers.^{43,44} Recently, the morphological transition of quantum dot/AB diblock copolymer hybrid micelles at different stirring rates was demonstrated by Zhang and co-workers.⁴⁵ Sorrells et al. focused on the influence of stirring rate on the shape and size alteration of ABC triblock copolymer micelles.⁴⁶ Such flow field is too chaotic to be mathematically described and cannot be compared with the simulation results. Considering the uniform shear rate (i.e., the shear rate on each lattice site is equal) used in the simulation, we prepared vesicles in a uniform shear field rather than in a chaotic shear field provided by a magnetic bar stirring at the bottom of a conical flask. To obtain

a uniform shear field, a Couette flow cell consisting of two concentric cylinders was fabricated. The gap between the cylinders was small enough relative to the radii of the cylinders so that the shear rate can be approximately considered to be identical everywhere in the gap. The shear rate only linearly depends on the angular frequency of the inner cylinder (see the Supporting Information).⁴⁷ In this Couette cell, vesicles formed by the ABA triblock copolymer $\text{P4VP}_{43}-b-\text{PS}_{366}-b-\text{P4VP}_{43}$ were obtained at different shear rates, as shown in Figure 5. Figure 5a shows that there are many large vesicles at low shear rate of 349 s^{-1} , the diameter of which ranges from 200 to 500 nm, mixing with relatively small vesicles within dozens of nanometers. As the shear rate increases, the large vesicles gradually become small and eventually disappear (Figures 5b,c), leaving only small vesicles (Figure 5d). This result correlates very well with the simulation results shown in Figure 2. Both simulative and experimental studies clearly indicate that the size of vesicles indeed decreases with increasing shear rate.

Additionally, the size uniformity of the vesicles is improved by increasing shear rate, which can be clearly seen in Figures 5a–c, especially in Figure 5d. The size distribution of the vesicles was investigated using dynamic light scattering (DLS).⁴⁸ The results are shown in Figure 6. The size distribution profile (Figure 6a) given by the CONTIN method shows that the size distribution narrows down as the shear rate increases. The hydrodynamic radius (R_h) and polydispersity index (PDI) obtained from the cumulant method are shown in Figure 6b. R_h decreases from 97 to 63 nm as the shear rate increases from 349 to 3489 s^{-1} . Meanwhile, the PDI decreases from 0.182 to 0.066. A smaller PDI value results in a narrower or more uniform size distribution of the vesicles. The very low PDI of 0.066 indicates that the vesicles at the shear rate of 3489 s^{-1} have an extremely narrow distribution and even can be regarded as monodisperse vesicles. As shown in Figure 5, the large vesicles disappear as the shear rate increases, leaving only small vesicles, which indicates that the size distribution narrows down. Thus, the DLS measurement results are consistent with the images (Figure 5) and the simulation results (Figures 3 and

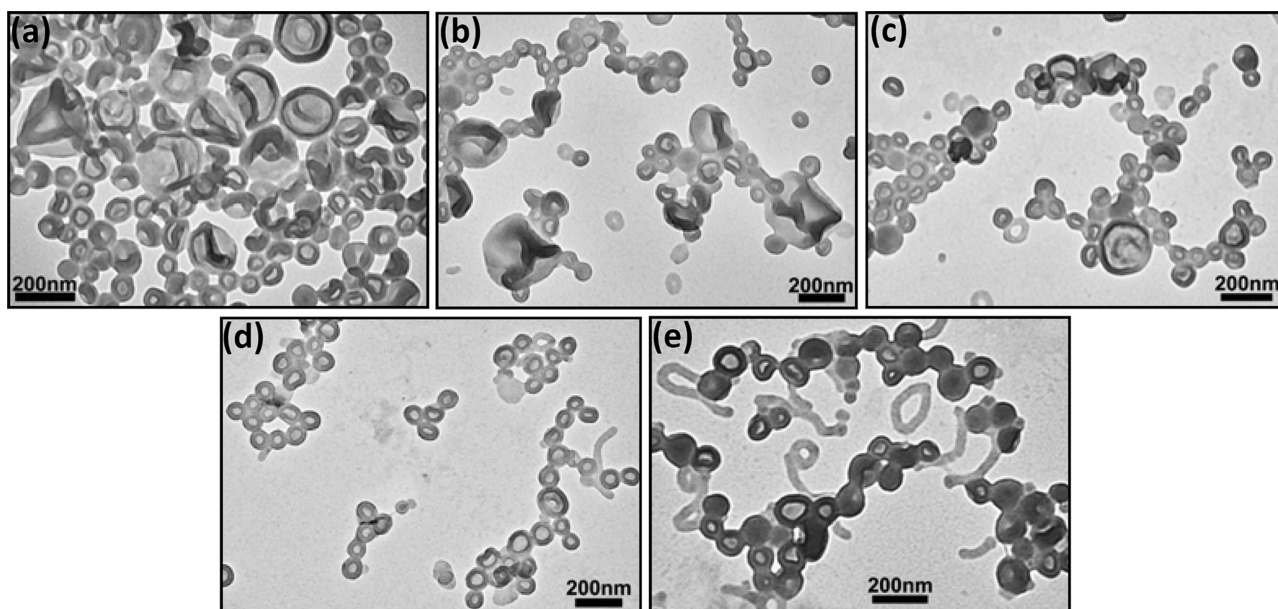


Figure 5. (a–d) TEM images of vesicles prepared in Couette flow cell at different shear rates of 349 , 872 , 2617 , and 3489 s^{-1} , respectively. (e) Aggregates obtained at 5233 s^{-1} .

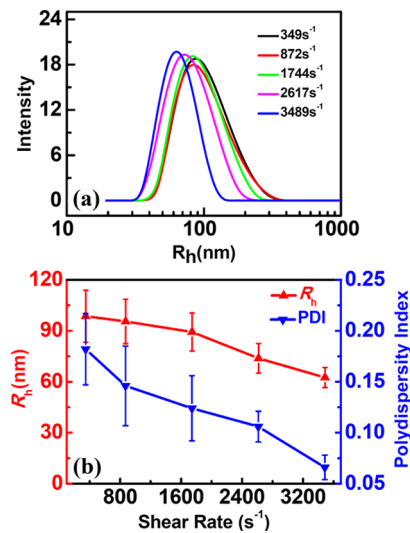


Figure 6. DLS measurement results of vesicles prepared in uniform shear field provided by Couette flow cell at different shear rates: (a) the size distribution curves given by the CONTIN method; (b) the R_h and PDI variation with shear rates given by the cumulant method.

4). The vesicle size distribution becomes narrower with the increase of shear rate.

On the other hand, it is worth to note that the highest shear rate used in this study is 3489 s⁻¹. We did not fabricate vesicles at shear rate higher than 3489 s⁻¹ for two reasons. First, the uniformity of the shear flow field depends on a relatively low shear rate. Turbulence in the shear flow field occurs if the shear rate exceeds a critical value and the shear field is no longer uniform.^{49,50} Second, other morphologies, such as spheres, short rods, and toroids, appear in the solution if the shear rate is high enough (5233 s⁻¹ in this study), as shown in Figure 5e. This finding is consistent with the simulation results shown in Figure 2e. Complex structures with short rods, spheres, and vesicles can be obtained from simulation when shear rate increases to 0.68. Therefore, the morphological polydispersity of amphiphilic ABA triblock copolymer vesicles can be considerably improved by increasing the shear rate within a wide range.

Finally, we calculated the energy from entropy (E_{entropy}), the energy from enthalpy (E_{enthalpy}), the energy from shear field (E_{shear}), and the total energy (E_{total} , the sum of these three energies), respectively, based on eqs 1 and 2.

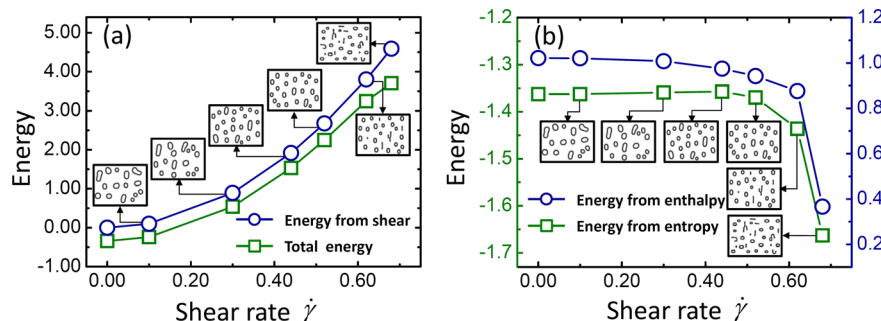


Figure 7. (a) Variations of the energy from shear E_{shear} and the total energy E_{total} with the shear rate. (b) Variations of the energy from entropy E_{entropy} and the energy from enthalpy E_{enthalpy} with the shear rate. For the purpose of convenience, morphological results corresponding to the shear rates are given.

$$\begin{aligned} E_{\text{entropy}} &= -f_p \ln(Q_p/f_p V) - N f_S \ln(Q_S/f_S V) \\ &\quad - 1/V \int d\vec{r} \left[\sum_{\alpha} \omega_{\alpha}(\vec{r}) \phi_{\alpha}(\vec{r}) + P(\vec{r})(1 - \sum_{\alpha} \phi_{\alpha}(\vec{r})) \right] \end{aligned} \quad (3)$$

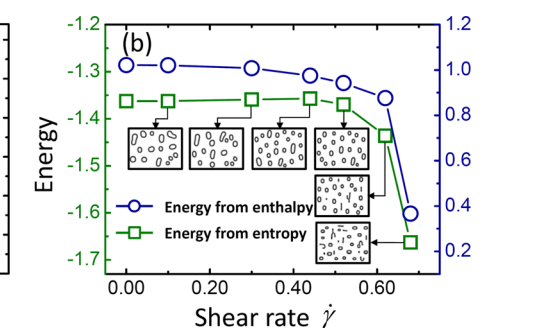
$$E_{\text{enthalpy}} = 1/V \int d\vec{r} \left[\sum_{\alpha \neq \beta} \chi_{\alpha\beta} N \phi_{\alpha}(\vec{r}) \phi_{\beta}(\vec{r}) / 2 \right] \quad (4)$$

$$E_{\text{shear}} = 1/V \int d\vec{r} \cdot \Delta G_{\text{shear}}(\vec{r}) \quad (5)$$

Figure 7 is the calculated results showing the variation of these energies with shear rate. For the purpose of convenience, morphological results corresponding to the shear rates are also given in Figure 7. From Figure 7a we can clearly see that both the E_{total} of the system and the E_{shear} increase monotonously with the increasing shear rate. Moreover, from the morphological results shown in Figure 7a it is clear that the averaged size of the self-assembled aggregates formed by the ABA copolymer decreases continuously with increasing shear rate. This indicates that the size of the self-assembled aggregates is mainly determined by the energy from the external shear field, i.e., E_{shear} . However, from Figure 7b it is seen that both the E_{entropy} and E_{enthalpy} remain almost unchanged with increasing shear rate up to 0.52; thereafter, it drops considerably. From the morphological results shown in Figure 7b it is clear that the morphology remains vesicle with increasing shear rate up to 0.52; thereafter, small sphere and short rod appear. This suggests that the morphology of the aggregate formed by the ABA block copolymer is mainly determined by the internal free energy of the system, i.e., $E_{\text{entropy}}+E_{\text{enthalpy}}$.

5. CONCLUSION

Previous studies have revealed that the existence of many metastable states not only determines the morphological polydispersity of polymeric assemblies^{23,34,35,51} but also determines its formation mechanism.⁵² The results in the present study indicate that the metastable states can be modulated and herein the polydispersity can be controlled by shear flow. This study provides a deeper insight into the metastable behavior of self-assembled polymeric aggregates and new information for solving the morphological polydispersity problem. The obtainment of uniform polymeric vesicles from this strategy may help to realize the full potential of these assemblies in many fields.



■ ASSOCIATED CONTENT

§ Supporting Information

Self-consistent field simulation method and Fabrication of Couette cell. This material is available free of charge via the Internet at <http://pubs.acs.org>.

■ AUTHOR INFORMATION

Corresponding Author

*Tel +86-431-85262151; Fax +86-431-85262126; e-mail wjiang@ciac.jl.cn (W.J.).

Notes

The authors declare no competing financial interest.

■ ACKNOWLEDGMENTS

We thank the financial support from the National Natural Science Foundation of China for Youth Science Funds (21104078) and Major Program (50930001).

■ REFERENCES

- (1) Zhang, L. F.; Eisenberg, A. Multiple Morphologies of Crew-cut Aggregates of Polystyrene-b-Poly(Acrylic Acid) Block-copolymers. *Science* **1995**, *268*, 1728–1731.
- (2) Discher, B. M.; Won, Y. Y.; Ege, D. S.; Lee, J. C. M.; Bates, F. S.; Discher, D. E.; Hammer, D. A. Polymersomes: Tough Vesicles Made from Diblock Copolymers. *Science* **1999**, *284*, 1143–1146.
- (3) Shen, H. W.; Eisenberg, A. Control of Architecture in Block-copolymer Vesicles. *Angew. Chem., Int. Ed.* **2000**, *39*, 3310–3312.
- (4) Discher, D. E.; Eisenberg, A. Polymer Vesicles. *Science* **2002**, *297*, 967–973.
- (5) Soo, P. L.; Eisenberg, A. Preparation of Block Copolymer Vesicles in Solution. *J. Polym. Sci., Polym. Phys.* **2004**, *42*, 923–938.
- (6) Bhargava, P.; Tu, Y. F.; Zheng, J. X.; Xiong, H. M.; Quirk, R. P.; Cheng, S. Z. D. Temperature-induced Reversible Morphological Changes of Polystyrene-block-Poly(Ethylene Oxide) Micelles in Solution. *J. Am. Chem. Soc.* **2007**, *129*, 1113–1121.
- (7) Kong, W. X.; Li, B. H.; Jin, Q. H.; Ding, D. T.; Shi, A. C. Helical Vesicles, Segmented Semivesicles, and Noncircular Bilayer Sheets from Solution-State Self-Assembly of ABC Miktoarm Star Terpolymers. *J. Am. Chem. Soc.* **2009**, *131*, 8503–8512.
- (8) Yu, S. Y.; Azzam, T.; Rouiller, I.; Eisenberg, A. “Breathing” Vesicles. *J. Am. Chem. Soc.* **2009**, *131*, 10557–10566.
- (9) Mai, Y.; Eisenberg, A. Self-assembly of Block Copolymers. *Chem. Soc. Rev.* **2012**, *41*, 5969–5985.
- (10) Moughton, A. O.; Hillmyer, M. A.; Lodge, T. P. Multicompartment Block Polymer Micelles. *Macromolecules* **2012**, *45*, 2–19.
- (11) Du, J. Z.; O'Reilly, R. K. Advances and Challenges in Smart and Functional Polymer Vesicles. *Soft Matter* **2009**, *5*, 3544–3561.
- (12) Kita-Tokarczyk, K.; Grumelard, J.; Haefele, T.; Meier, W. Block Copolymer Vesicles—Using Concepts from Polymer Chemistry to Mimic Biomembranes. *Polymer* **2005**, *46*, 3540–3563.
- (13) Sahoo, S. K.; Labhasetwar, V. Nanotech Approaches to Delivery and Imaging Drug. *Drug Discovery Today* **2003**, *8*, 1112–1120.
- (14) Kataoka, K.; Harada, A.; Nagasaki, Y. Block Copolymer Micelles for Drug Delivery: Design, Characterization and Biological Significance. *Adv. Drug Delivery Rev.* **2001**, *47*, 113–131.
- (15) LoPresti, C.; Lomas, H.; Massignani, M.; Smart, T.; Battaglia, G. Polymersomes: Nature Inspired Nanometer Sized Compartments. *J. Mater. Chem.* **2009**, *19*, 3576–3590.
- (16) Brinkhuis, R. P.; Rutjes, F.; van Hest, J. C. M. Polymeric Vesicles in Biomedical Applications. *Polym. Chem.* **2011**, *2*, 1449–1462.
- (17) Carstens, M. G.; Camps, M. G. M.; Henriksen-Lacey, M.; Franken, K.; Ottenhoff, T. H. M.; Perrie, Y.; Bouwstra, J. A.; Ossendorp, F.; Jiskoot, W. Effect of Vesicle Size on Tissue Localization and Immunogenicity of Liposomal DNA Vaccines. *Vaccine* **2011**, *29*, 4761–4770.
- (18) Rao, J. P.; Geckeler, K. E. Polymer Nanoparticles: Preparation Techniques and Size-Control Parameters. *Prog. Polym. Sci.* **2011**, *36*, 887–913.
- (19) Lee, J. S.; Feijen, J. Polymersomes for Drug Delivery: Design, Formation and Characterization. *J. Controlled Release* **2012**, *161*, 473–483.
- (20) Letchford, K.; Burt, H. A Review of the Formation and Classification of Amphiphilic Block Copolymer Nanoparticulate Structures: Micelles, Nanospheres, Nanocapsules and Polymersomes. *Eur. J. Pharm. Biopharm.* **2007**, *65*, 259–269.
- (21) Burke, S.; Shen, H. W.; Eisenberg, A. Multiple Vesicular Morphologies from Block Copolymers in Solution. *Macromol. Symp.* **2001**, *175*, 273–283.
- (22) Kim, K. T.; Zhu, J. H.; Meeuwissen, S. A.; Cornelissen, J.; Pochan, D. J.; Nolte, R. J. M.; van Hest, J. C. M. Polymersome Stomatocytes: Controlled Shape Transformation in Polymer Vesicles. *J. Am. Chem. Soc.* **2010**, *132*, 12522–12524.
- (23) Zhu, J. T.; Jiang, Y.; Liang, H. J.; Jiang, W. Self-Assembly of ABA Amphiphilic Triblock Copolymers into Vesicles in Dilute Solution. *J. Phys. Chem. B* **2005**, *109*, 8619–8625.
- (24) Howse, J. R.; Jones, R. A. L.; Battaglia, G.; Ducker, R. E.; Leggett, G. J.; Ryan, A. J. Templated Formation of Giant Polymer Vesicles with Controlled Size Distributions. *Nat. Mater.* **2009**, *8*, 507–511.
- (25) Jung, H. T.; Coldren, B.; Zasadzinski, J. A.; Iampietro, D. J.; Kaler, E. W. The Origins of Stability of Spontaneous Vesicles. *Proc. Natl. Acad. Sci. U. S. A.* **2001**, *98*, 1353–1357.
- (26) Battaglia, G.; Ryan, A. J. Bilayers and Interdigitation in Block Copolymer Vesicles. *J. Am. Chem. Soc.* **2005**, *127*, 8757–8764.
- (27) Brown, L.; McArthur, S. L.; Wright, P. C.; Lewis, A.; Battaglia, G. Polymersome Production on a Microfluidic Platform Using pH Sensitive Block Copolymers. *Lab Chip* **2010**, *10*, 1922–1928.
- (28) Dong, W. F.; Kishimura, A.; Anraku, Y.; Chuano, S.; Kataoka, K. Monodispersed Polymeric Nanocapsules: Spontaneous Evolution and Morphology Transition from Reducible Hetero-PEG PICmicelles by Controlled Degradation. *J. Am. Chem. Soc.* **2009**, *131*, 3804–3805.
- (29) Holowka, E. P.; Pochan, D. J.; Deming, T. J. Charged Polypeptide Vesicles with Controllable Diameter. *J. Am. Chem. Soc.* **2005**, *127*, 12423–12428.
- (30) Lomas, H.; Massignani, M.; Abdullah, K. A.; Canton, I.; Lo Presti, C.; MacNeil, S.; Du, J. Z.; Blanazs, A.; Madsen, J.; Armes, S. P.; Lewis, A. L.; Battaglia, G. Non-cytotoxic Polymer Vesicles for Rapid and Efficient Intracellular Delivery. *Faraday Discuss.* **2008**, *139*, 143–159.
- (31) Shum, H. C.; Kim, J. W.; Weitz, D. A. Microfluidic Fabrication of Monodisperse Biocompatible and Biodegradable Polymersomes with Controlled Permeability. *J. Am. Chem. Soc.* **2008**, *130*, 9543–9549.
- (32) Xu, W. J.; Yu, X.; Liang, R. J.; Liu, S. Q.; Tian, Q. W.; Deng, R. H.; Zhu, J. T. Generation of Polymer Nanocapsules via a Membrane-extrusion Emulsification Approach. *Mater. Lett.* **2012**, *77*, 96–99.
- (33) Zhang, L. F.; Eisenberg, A. Formation of Crew-cut Aggregates of Various Morphologies from Amphiphilic Block Copolymers in Solution. *Polym. Adv. Technol.* **1998**, *9*, 677–699.
- (34) He, X. H.; Liang, H. J.; Huang, L.; Pan, C. Y. Complex Microstructures of Amphiphilic Diblock Copolymer in Dilute Solution. *J. Phys. Chem. B* **2004**, *108*, 1731–1735.
- (35) Jiang, Y.; Zhu, J. T.; Jiang, W.; Liang, H. J. Cornucopian Cylindrical Aggregate Morphologies from Self-Assembly of Amphiphilic Triblock Copolymer in Selective Media. *J. Phys. Chem. B* **2005**, *109*, 21549–21555.
- (36) Greenall, M. J.; Marques, C. M. Can Amphiphile Architecture Directly Control Vesicle Size? *Phys. Rev. Lett.* **2013**, *110*, 088301.
- (37) Derolet, F.; Fredrickson, G. H. Combinatorial Screening of Complex Block Copolymer Assembly with Self-consistent Field Theory. *Phys. Rev. Lett.* **1999**, *83*, 4317–4320.
- (38) Derolet, F.; Fredrickson, G. H. Optimizing Chain Bridging in Complex Block Copolymers. *Macromolecules* **2001**, *34*, 5317–5324.

- (39) Fredrickson, G. H.; Ganesan, V.; Drolet, F. Field-Theoretic Computer Simulation Methods for Polymers and Complex Fluids. *Macromolecules* **2002**, *35*, 16–39.
- (40) An, L. J.; Wolf, B. A. Combined Effects of Pressure and Shear on the Phase Separation of Polymer Solutions. *Macromolecules* **1998**, *31*, 4621–4625.
- (41) Sun, Z. Y.; Yang, J. A.; Jiang, W.; An, L. J.; Jiang, Z. H.; Wu, Z. W. Theoretical Representation of Shear and Pressure Influence on the Phase Separation Behavior of PVME/PS Mixture. *Polymer* **2002**, *43*, 4047–4054.
- (42) Yu, H. Z.; Zhu, J. T.; Jiang, W. Effect of Binary Block-Selective Solvents on Self-Assembly of ABA Triblock Copolymer in Dilute Solution. *J. Polym. Sci., Polym. Phys.* **2008**, *46*, 1536–1545.
- (43) Yu, H. Z.; Jiang, W. Effect of Shear Flow on the Formation of Ring-Shaped ABA Amphiphilic Triblock Copolymer Micelles. *Macromolecules* **2009**, *42*, 3399–3404.
- (44) Wang, Z.; Jiang, W. Temperature-Induced Reversible Transformation between Toroidal and Cylindrical Assemblies under Shear Flow. *Soft Matter* **2010**, *6*, 3743–3746.
- (45) Zhang, M.; Wang, M. F.; He, S.; Qian, J. S.; Saffari, A.; Lee, A.; Kumar, S.; Hassan, Y.; Guenther, A.; Scholes, G.; Winnik, M. A. Sphere-to-Wormlike Network Transition of Block Copolymer Micelles Containing CdSe Quantum Dots in the Corona. *Macromolecules* **2010**, *43*, 5066–5074.
- (46) Sorrells, J. L.; Tsai, Y. H.; Wooley, K. L. The Influence of Solution-State Conditions and Stirring Rate on the Assembly of Poly(acrylic acid)-Containing Amphiphilic Triblock Copolymers with Multi-Amines. *J. Polym. Sci., Polym. Chem.* **2010**, *48*, 4465–4472.
- (47) Nguyen, Q. D.; Boger, D. V. Characterization of Yield Stress Fluids with Concentric Cylinder Viscometers. *Rheol. Acta* **1987**, *26*, 508–515.
- (48) Berne, B. J.; Pecora, R. *Dynamic Light Scattering: With Applications to Chemistry, Biology, and Physics*; Wiley: New York, 1976.
- (49) Recktenwald, A.; Lucke, M.; Muller, H. W. Taylor Vortex Formation in Axial Through-Flow: Linear and Weakly Nonlinear Analysis. *Phys. Rev. E* **1993**, *48*, 4444–4454.
- (50) Batten, W. M. J.; Turnock, S. R.; Bressloff, N. W.; Abu-Sharkh, S. M. Turbulent Taylor-Couette Vortex Flow between Large Radius Ratio Concentric Cylinders. *Exp. Fluids* **2004**, *36*, 419–421.
- (51) Ortiz, V.; Nielsen, S. O.; Klein, M. L.; Discher, D. E. Computer Simulation of Aqueous Block Copolymer Assemblies: Length Scales and Methods. *J. Polym. Sci., Polym. Phys.* **2006**, *44*, 1907–1918.
- (52) Han, Y. Y.; Yu, H. Z.; Du, H. B.; Jiang, W. Effect of Selective Solvent Addition Rate on the Pathways for Spontaneous Vesicle Formation of ABA Amphiphilic Triblock Copolymers. *J. Am. Chem. Soc.* **2010**, *132*, 1144–1150.